Research Article | Vol. 25, No. 21 | 16 Oct 2017 | OPTICS EXPRESS 26118
Optics EXPRESS

Transition between bulk and surface refractive index sensitivity of micro-cavity in-line Mach-Zehnder interferometer induced by thin film deposition

MATEUSZ ŚMIETANA,[1,*] MONIKA JANIK,[2] MARCIN KOBA,[1,3] AND WOJTEK J. BOCK[2]

[1]*Institute of Microelectronics and Optoelectronics, Warsaw University of Technology, Koszykowa 75, Warsaw 00-662, Poland*
[2]*Centre de recherche en photonique, Université du Québec en Outaouais, 101 rue Saint-Jean-Bosco, Gatineau, QC, J8X 3X7, Canada*
[3]*National Institute of Telecommunications, Szachowa 1, Warsaw, 04-894, Poland*
**M.Smietana@elka.pw.edu.pl*

Abstract: In this work we discuss the refractive index (RI) sensitivity of a micro-cavity in-line Mach-Zehnder interferometer in the form of a cylindrical hole (40-50 μm in diameter) fabricated in a standard single-mode optical fiber using a femtosecond laser. The surface of the micro-cavity was coated with up to 400 nm aluminum oxide thin film using the atomic layer deposition method. Next, the film was progressively chemically etched and the influence on changes in the RI of liquid in the micro-cavity was determined at different stages of the experiment, i.e., at different thicknesses of the film. An effect of transition between sensitivity to the film thickness (surface) and the RI of liquid in the cavity (bulk) is demonstrated for the first time. We have found that depending on the interferometer working conditions determined by thin film properties, the device can be used for investigation of phenomena taking place at the surface, such as in case of specific label-free biosensing applications, or for small-volume RI analysis as required in analytical chemistry.

OCIS codes: (280.4788) Optical sensing and sensors; (060.2370) Fiber optics sensors; (220.4000) Microstructure fabrication; (230.3990) Micro-optical devices; (120.3180) Interferometry; (240.0310) Thin films.

References and links

1. M. Pospíšilová, G. Kuncová, and J. Trögl, "Fiber-Optic Chemical Sensors and Fiber-Optic Bio-Sensors," Sensors (Basel) **15**(10), 25208–25259 (2015).
2. E. Brzozowska, M. Śmietana, M. Koba, S. Górska, K. Pawlik, A. Gamian, and W. J. Bock, "Recognition of bacterial lipopolysaccharide using bacteriophage-adhesin-coated long-period gratings," Biosens. Bioelectron. **67**, 93–99 (2015).
3. S. Lepinay, A. Staff, A. Ianoul, and J. Albert, "Improved detection limits of protein optical fiber biosensors coated with gold nanoparticles," Biosens. Bioelectron. **52**, 337–344 (2014).
4. R. Różycki-Bakon, M. Koba, P. Firek, E. Roźniecka, J. Niedziółka-Jonsson, and M. Śmietana, "Stack of nano-films on optical fiber end-face for label-free bio-recognition," J. Lightwave Technol. **34**, 5357–5362 (2016).
5. M. Dominik, A. Leśniewski, M. Janczuk, J. Niedziółka-Jönsson, M. Hołdyński, Ł. Wachnicki, M. Godlewski, W. J. Bock, and M. Śmietana, "Titanium oxide thin films obtained with physical and chemical vapour deposition methods for optical biosensing purposes," Biosens. Bioelectron. **93**, 102–109 (2017).
6. M. Smietana, M. Koba, E. Brzozowska, K. Krogulski, J. Nakonieczny, L. Wachnicki, P. Mikulic, M. Godlewski, and W. J. Bock, "Label-free sensitivity of long-period gratings enhanced by atomic layer deposited TiO2 nano-overlays," Opt. Express **23**(7), 8441–8453 (2015).
7. F. He, Y. Liao, J. Lin, J. Song, L. Qiao, Y. Cheng, and K. Sugioka, "Femtosecond Laser Fabrication of Monolithically Integrated Microfluidic Sensors in Glass," Sensors (Basel) **14**(10), 19402–19440 (2014).
8. K. Goya, T. Itoh, A. Seki, and K. Watanabe, "Efficient deep-hole drilling by a femtosecond, 400 nm secondharmonic Ti:Sapphire laser for a fiber optic in-line/pico-literspectrometer," Sens. Actuat. B **210**, 685–691 (2015).
9. L. Jiang, L. Zhao, S. Wang, J. Yang, and H. Xiao, "Femtosecond laser fabricated all-optical fiber sensors with ultrahigh refractive index sensitivity: modeling and experiment," Opt. Express **19**(18), 17591–17598 (2011).

#304077 https://doi.org/10.1364/OE.25.026118
Journal © 2017 Received 4 Aug 2017; revised 4 Oct 2017; accepted 6 Oct 2017; published 12 Oct 2017

Optics EXPRESS

10. M. Janik, A. K. Myśliwiec, M. Koba, A. Celebańska, W. J. Bock, and M. Smietana, "Sensitivity Pattern of Femtosecond Laser Micromachined and Plasma-Processed In-Fiber Mach-Zehnder Interferometers, as Applied to Small-Scale Refractive Index Sensing," IEEE Sensors **17**, 3316–3322 (2017).
11. Z. Li, C. Liao, D. Chen, J. Song, W. Jin, G.-D. Peng, F. Zhu, Y. Wang, J. He, and Y. Wang, "Label-free detection of bovine serum albumin based on an in-fiber Mach-Zehnder interferometric biosensor," Opt. Express **25**(15), 17105–17113 (2017).
12. M. Smietana, M. Mysliwiec, P. Mikulic, B. S. Witkowski, and W. J. Bock, "Capability for fine tuning of the refractive index sensing properties of long-period gratings by atomic layer deposited Al_2O_3 overlays," Sensors (Basel) **13**(12), 16372–16383 (2013).
13. M. Śmietana, M. Koba, P. Mikulic, and W. J. Bock, "Towards refractive index sensitivity of long-period gratings at level of tens of μm per refractive index unit: fiber cladding etching and nano-coating deposition," Opt. Express **24**(11), 11897–11904 (2016).
14. A. I. Abdulagatov, Y. Yan, J. R. Cooper, Y. Zhang, Z. M. Gibbs, A. S. Cavanagh, R. G. Yang, Y. C. Lee, and S. M. George, "Al2O3 and TiO2 Atomic Layer Deposition on Copper for Water Corrosion Resistance," ACS Appl. Mater. Interfaces **3**(12), 4593–4601 (2011).
15. J. Oh, J. Myoung, J. S. Bae, and S. Lim, "Etch Behavior of ALD Al2O3 on HfSiO and HfSiON Stacks in Acidic and Basic Etchants," J. Electrochem. Soc. **158**(4), D217–D222 (2011).
16. M. Koba, M. Śmietana, E. Brzozowska, S. Górska, M. Janik, A. Gamian, P. Mikulic, A. Cusano, and W. J. Bock, "Bacteriophage Adhesin-Coated Long-Period Grating-Based Sensor: Bacteria Detection Specificity," J. Lightwave Technol. **34**, 4531–4536 (2016).

1. Introduction

Optical sensors offer many advantages, such as capability for real-time monitoring of reaction kinetics, immunity to electromagnetic interference, and ability to function in corrosive and harsh environments. A number of liquids significantly change their optical properties when contaminated as well as undergoing thermal or oxidation processing. Analysis of such phenomena is demanded in the food and chemical industries and is typically done using refractometers, which determine the refractive index (RI) of the liquids. When the liquids contain biological molecules, the molecules may bind to the surface and significantly change optical properties only in close proximity to the surface. This sensing phenomenon is often employed for label-free sensing, where in the case of optical measurements it corresponds to specific growth of a biological layer with increased RI [1]. In this sensing concept, specificity of detection (selectivity) is determined by surface functionalization so that only certain target molecules are bound. The sensitivity depends mainly on the properties of the applied device. Liquids containing biomolecules are typically available only in small or very small volumes, and their analysis is required in molecular biology or prevention of terrorism.

For sensors based on optical fibers, in addition to the advantages mentioned above, a probe-like sensor shape and the capability of remote and multi-parameter sensing are available. The label-free sensing concept has already been applied to a number of optical-fiber-based devices. The most widely explored in this respect are long-period gratings [2], tilted fiber Bragg gratings [3], various interferometers [4], and combinations of those with thin films [5], which induce or modify RI sensitivity. For some of these sensing architectures, there is close correspondence between an applied quantity of liquid (bulk) and a thin layer of biomolecules (surface) in terms of high RI sensitivity [6].

Optical fiber structures based on a micro-cavity can be considered as a relatively new class of sensing devices. They are most often fabricated using femtosecond (fs) laser ablation. Thanks to sub-micrometer precision of this technique, cavities of various shapes and sizes can be made, e.g., in a telecom optical fiber [7]. When the cavity is significantly deeper than the fiber radius, the device can be applied as a spectroscopic micro-cuvette [8], but if it only slightly interacts with the fiber core, a Mach-Zehnder (MZ) interferometer can be obtained [9]. The cavity wall acts as a beam splitter, where one beam propagates in the core and the other penetrates the cavity. The beams interfere at the second cavity wall. Depending on the cavity dimensions, different interference patterns can be obtained on the fiber output. It has been shown that when the shift of wavelength corresponding to the transmission minima vs. RI is considered, sensing structures of this type may offer RI sensitivity reaching over 20.000 nm/RIU [10]. A bulk RI sensitivity is defined in this case for the medium filling the cavity

Optics EXPRESS

[11]. However, such devices have never been applied for specific towards certain molecules label-free sensing, where only changes in RI at the sensor surface need to be investigated.

In this work we show an effect of transition between bulk and surface RI sensitivities of an fs-laser-fabricated micro-cavity in-line MZ interferometer (μIMZI) when coated with high-RI film. Surface sensitivity was investigated by deposition of aluminum oxide (Al_2O_3) inside the micro-cavity using the atomic layer deposition (ALD) method followed by its slow chemical etching. We show that depending on the μIMZI working point determined by the thin film properties, here mainly the thickness and RI, the device can be used for investigation of phenomena taking place at the surface, such as in case of specific label-free biosensing applications, or for small-volume RI analysis as required in analytical chemistry.

2. Experimental details

2.1 The μIMZI fabrication

The micro-cavities were fabricated in a single-mode fiber (Corning SMF28) using a Solstice Ti:Sapphire fs laser operating at λ = 795 nm with a repetition rate of 10 kHz [10], and average power of 4 W. The fiber was irradiated by 82 fs pulses and the laser beam with only a fraction of its averaged power was directed into a suitably designed micromachining setup based on the Newport μFab system equipped with a 20x lens (NA = 0.30). The diameter of the cavity was set to 40 and 50 μm. Progress of the fabrication was controlled by monitoring fiber transmission during the process in the wavelength range 1100-1700 nm with a NKT Photonics SuperK COMPACT supercontinuum white-light source and a Yokogawa AQ6370C optical spectrum analyzer supported by a software developed in-house. Taking into account a long term light source stability, accuracy of the spectrum analyzer, and the high repeatability and stability of a single sensor, the overall accuracy of the measurements was estimated at the level of 0.7 nm in terms of wavelength and +/– 0.6 dB in terms of power.

2.2 Thin film deposition

The Al_2O_3 films were deposited on both the μIMZI and the reference silicon wafers by the ALD method using the Cambridge NanoTech Savannah S100 system according to the procedure described in [12]. For the deposition process, water and trimethylaluminum (TMA, $Al(CH_3)_3$) precursors were used. Thickness (t) of the Al_2O_3 film was controlled by the number of ALD cycles that reached 4000. Thickness and optical properties of the films deposited on the reference Si wafers were determined using ellipsometry with a procedure described in [13]. The representation of the investigated structure is shown in Fig. 1.

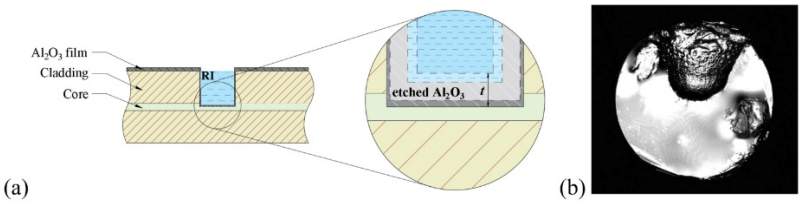

Fig. 1. Investigated μIMZI structure, where (a) shows it schematically with thin Al_2O_3 film when filled with liquid and (b) shows microscopic image of its cross-section. During the experiment slow chemical etching of the Al_2O_3 thin film in the cavity took place. In (a) arrow indicates the thickness t of the etched layer. In (b) the feature on the right is a cut residue.

2.3 RI sensitivity measurements

The Al_2O_3 thickness was reduced by filling the cavity with sodium hydroxide (NaOH) of known concentration (10 mM and 1 M) at a fixed temperature (T = 20°C) for a specified time, followed by extensive washing with deionized water. The optical transmission spectrum of the μIMZI was investigated and compared when the cavity was filled with deionized water, as

Optics EXPRESS

well as at arbitrary stages of the etching process for RI changes in the cavity in the range n_D = 1.3330 to 1.3999 RIU. Liquids of various RI values were prepared as a mixture of deionized water and glycerine, and verified using a VEE GEE PDX-95 digital refractometer working with a resolution of 10^{-4} RIU. Before the first NaOH etching the cavity underwent 30 s of oxygen plasma processing, which increased the wettability of the film surface and made it possible to fill the cavity with the liquids [10].

3. Results and discussion

The ALD process used in this experiment allows for outstanding control over the properties of the deposited film [12, 13]. Commonly deposited with ALD, Al_2O_3 is often applied as a mechanically protective or electrically passivating coating [14]. However, Al_2O_3 is an amphoteric material that can be dissolved in both highly concentrated acids and alkalis [15]. It has been determined on reference samples using spectroscopic ellipsometry that the deposition and etching rates of Al_2O_3 in 10 mM NaOH reached ~0.1 nm/cycle and ~0.65 nm/min, respectively. Influence of the etching process on the spectral response of the μIMZI (d = 40 μm) is shown in Fig. 2. The cavity was coated with film having a thickness of t = 397 nm. Since the RI of Al_2O_3 is higher than that of either the fiber core or the cladding [12], the coating may simulate the device to increase the RI at the cavity surface, as is the case with biological film formation [16]. The experiment allows for estimation of the surface RI sensitivity of the device vs. t of the high-RI film, or eventually a biological film growth. In general, during the entire experiment the transmission minima shift towards shorter wavelengths with a decrease in t of the thin film. The shift intensifies after ~50 min of etching and reaches 2 and 4.7 nm/min respectively for minima (I) appearing below 1220 and (II) appearing above 1300 nm. It must be noted that the shift of minimum (II) is the highest there, but could not be monitored in the applied spectral range from the beginning of the experiment. After ~120 min of etching, minimum (I) is no longer visible in the investigated spectral range, while minimum (II) slows down its wavelength shift and starts to significantly change its transmission curve. When the etching process exceeds ~180 min up to about 320 min, the spectral response changes very little. Hardly any etching effect was observable from the moment we increased the NaOH etching concentration to 1 M, which corresponds to an etching rate of more than 4 nm/min according to ellipsometric measurements made on the reference Si samples. For etching in this range, there was no noticeable shift in wavelength, only a decrease in transmission by 10 dB towards the spectral response recorded before the deposition.

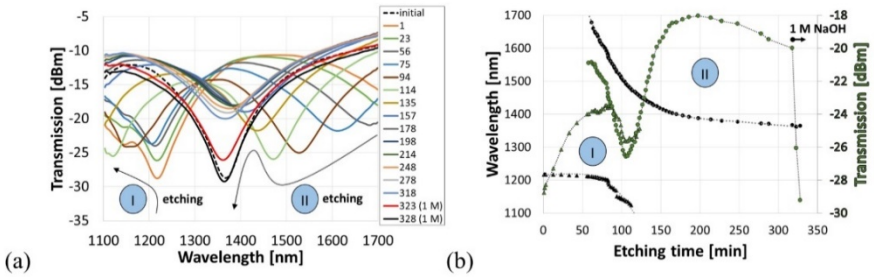

Fig. 2. Response of the μIMZI to Al_2O_3 film etching recorded for water-filled cavity, where (a) shows evolution of the transmission spectrum during the process in reference to the response before deposition and (b) plots wavelengths and transmission corresponding to local minima (I) and (II). After 323 minutes of etching in 10 mM NaOH, due to low process effectiveness the solution was replaced with 1 M NaOH.

In summary, when the wavelength of the transmission minimum is used for sensing purposes and when the etching rates are assumed to be directly related to those of the films deposited in the cavities, the surface sensitivity is the highest for Al_2O_3 film thicknesses

Optics EXPRESS

between 300 and 350 nm, where 1 nm decrease in *t* corresponds to ~3 nm shift of the transmission minimum. The effect potentially allows for sub-nm monitoring of changes in thickness at the sensor surface. When transmitted power at the minimum is interrogated, three *t* ranges can be listed where the sensitivity is increased up to ~0.2 dB/nm, namely approx. 330-340 nm, 290-320 nm and below 50 nm.

In order to estimate the influence of *t* on bulk RI sensitivity, at selected arbitrary stages of the etching process the response of the structure to variations of RI in the cavity was measured. In general, the transmission minima shift towards shorter wavelengths with bulk RI in the cavity (Fig. 3a). Minimum (II) is observed in the RI range from 1.3330 up to 1.37 RIU, where for higher RI it shifts below the interrogated spectral range (Fig. 3b). Next, a minimum (III) appears at a longer wavelength and can be traced for RI above 1.37 RIU. It can be seen that the bulk RI sensitivity strongly depends on *t* as well: the thicker the Al_2O_3 film, the lower the bulk RI sensitivity. It varies from about 5,430 to 12,390 nm/RIU and 9,090 to 18,000 nm/RIU for transmission minima (II) and (III), respectively.

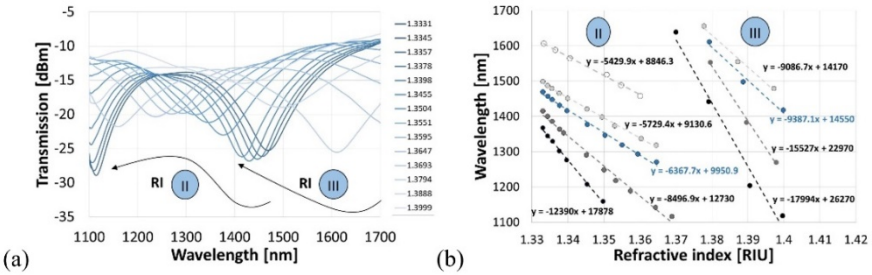

Fig. 3. Effect of increase in RI of liquid in the micro-cavity for different thicknesses of the Al_2O_3 film, where (a) shows spectral response at a selected stage of the etching experiment and (b) gives a summary of the measurements with determined sensitivity at each stage of etching. In (b) the measurement points marked in blue correspond to results shown in (a).

The results shown above indicate the significant influence of a thin film deposited in the cavity on both the surface and the bulk RI sensitivity of the investigated μIMZI. In order to verify whether the cavity depth induces an effect in the same way as depositing a high-RI thin film, we made four μIMZI structures (d = 50 μm) with spectral responses to water as shown in Fig. 4a. The only difference between the structures was their depth, where the deepest had the highest insertion losses.

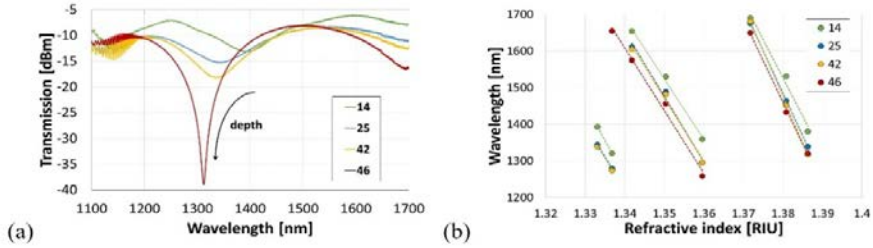

Fig. 4. Influence of the cavity depth (different amount of fs laser runs) on spectral response to RI, where (a) shows initial spectra for cavity filled with water and (b) shows wavelength shift of minima with RI. Diameter of the cavity was d = 50 μm.

It can be seen that increasing the cavity depth induces a spectral shift of the minimum towards a shorter wavelength. The effect in terms of direction of the shift corresponds to the decrease in *t*. However, fabrication of more shallow cavities, which may correspond to higher *t*, resulted in the complete absence of any transmission minimum, so obtaining results such as shown in Fig. 2a was impossible when the cavity had no film coating. Moreover, the depth of the cavity had no significant influence on the bulk RI response as shown in Fig. 4b. The most

Optics EXPRESS

significant difference between the responses for different cavity depths is how easy it is to determine the wavelength corresponding to the transmission minimum and to detect the left shift which are both most evident for the deepest cavity.

It must be noted that increasing the RI in the cavity by adding either a high-RI film or a liquid, produces opposite responses observed at the μIMZI output, i.e., shifts of the spectrum towards longer and shorter wavelengths, respectively. Following the analysis presented in [11] and Eq. (1), in which the wavelength corresponding to each transmission minimum (λ_m) is expressed by cavity diameter (d), an initial phase (φ_0), and the difference between the effective indices of the two interfering modes $\Delta n_{eff} = n_{eff}^{co} - n^{cl}$, where the remaining part of the fiber core corresponds to n_{eff}^{co} and that of the circular cavity to n^{cl}.

$$\lambda_m = \frac{2\pi d \Delta n_{eff}}{(2m+1)\pi - \varphi_0}, \tag{1}$$

In the case of RI sensitivity, the response of the μIMZI relies mainly on Δn_{eff}. Thus, when the liquid RI is increased, the propagation conditions are mainly affected through n^{cl} and the characteristic minimum then shifts towards shorter wavelengths. In turn, when a high-RI film is grown on the core surface, the $n^{co}{}_{eff}$ is changed while the n^{cl} stays generally unchanged, and the minima shift towards longer wavelengths. These circumstances explain why the measured responses to the surface and bulk RI are opposite. Moreover, there is a certain range of t where the sensitivity of the μIMZI to changes in the overlay is high. Within this range, any surface change, especially any change of t, strongly impacts $n^{co}{}_{eff}$ yet has a negligible influence on propagation in the cavity. This unique range of thicknesses should be applied when high surface RI sensitivity is expected, e.g., in bio-specific measurements.

4. Conclusions

In this work we show for the first time the possibility of transition between bulk and surface RI sensitivity of a μIMZI by application of thin high-RI film in the cavity. When there is no film in the cavity, the sensor is highly sensitive to the RI of liquid in the cavity and as already reported can be used to investigate small volumes of liquids [10]. In such working conditions the sensor may only slightly react, mainly by a change in transmission, to formation of the thin film on the cavity surface. However, when a thin high-RI film of a certain thickness is deposited in the cavity, the device significantly responds to any variation in the thin film thickness with a wavelength shift. This response can be used to identify the presence of a biological film growth. For these conditions the bulk RI sensitivity is lower than for the uncoated μIMZI. It is also to be expected that for thick biological films, such as bacteria-based films, change in the bio-layer thickness can be investigated with no interfacial film. We believe that the sensitivity transition effect can also be obtained with other thin films, especially those with very high RI. Such films are likely to be deposited thinner, i.e., through a shorter deposition process, to support a similar transition effect. Depending on the intended application, the μIMZI device can then be used for bulk or surface RI sensing. The approach is very promising given the high RI sensitivity and very low temperature sensitivity of this device.

Funding

National Science Centre, Poland (NCN) (2014/13/B/ST7/01742); the Canada Research Chairs Program, and the Natural Sciences and Engineering Research Council of Canada.